Critical instrumentation issues for <2 mm resolution, high sensitivity brain PET*†

Stephen E. Derenzo, William W. Moses, Ronald H. Huesman, and Thomas F. Budinger

Lawrence Berkeley Laboratory, University of California, Berkeley, CA 94720

ABSTRACT

This paper reviews critical developments in instrumentation necessary to achieve a resolution finer than 2 mm full-width at half-maximum (fwhm) in all three dimensions, a maximum event rate limited by patient dose rather than system dead time, and a detection sensitivity close to the theoretical limit.

INTRODUCTION

In the last 30 years, enormous advances have been made in the spatial resolution, detection sensitivity, and count rate capability of PET detectors [1-62]. In this paper we describe the critical instrumentation issues for future advances, which are necessary to improve the ability to study flow, metabolism, and neurochemistry in specific brain structures such as the sublayers of the cortex and important nuclei.

SPATIAL RESOLUTION

Detector size.

Until recently, the largest contribution to spatial resolution has been the detector size *d*. In the newer high resolution positron tomographs, where *d* is below 3 mm, other factors such as noncollinearity and light sharing statistics become important. However, efficiently stopping 511 keV photons in small crystals can be accomplished only by photoelectric absorption. Compton scattering, useful in large crystals, causes energy depositions in two or more small crystals typically 1-2 cm apart. High resolution PET needs detector materials with good stopping power, not good scattering power. This concept is illustrated in Figure 1, where the square of the ratio of photoelectric cross section to the sum of the photoelectric and Compton cross sections is plotted as a function of atomic number. This quantity is the coincident probability of photoelectric absorption of both 511 keV annihilation photons on the first interaction. All high resolution (<4 mm fwhm) positron tomographs use BGO ($Bi_4Ge_3O_{12}$) as the detector material [63-65].

* Work supported in part by the U.S. Department of Energy under Contract No. DE-AC03-76SF00098, in part by U.S. NIH grants R01-CA48002, P01-HL25840, and R01-NS29655, and in part by a grant from the Whitaker Foundation.

†Published in the book *Quantification of Brain Function*. Amsterdam, The Netherlands: Elsevier Science Publishers, 1993, pp 25-37.

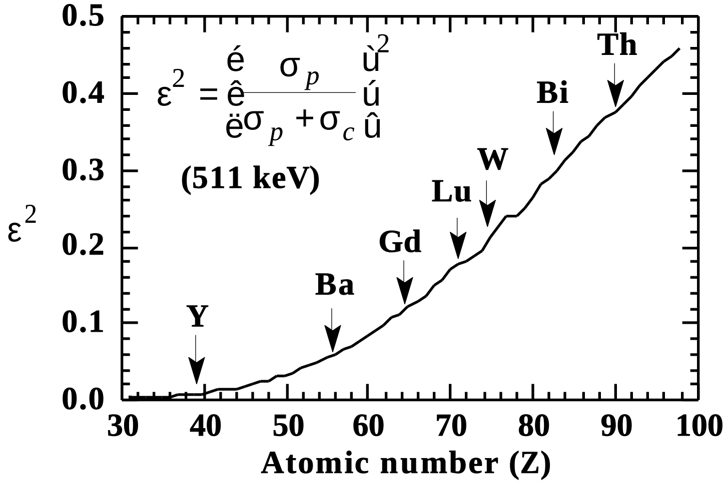

Figure 1.
Probability of coincident photoelectric absorption on the first interaction for 511 keV photons interacting with elements of atomic number Z.

Noncollinearity.

Because the positrons do not come to a complete rest before annihilation, the two 511 keV annihilation photons are not emitted in exactly opposite directions [66]. The result is a Gaussian angular distribution with about 0.5° fwhm. At the center of the tomograph, this translates to a contribution of 0.0022*D*, where *D* is the detector ring diameter.

Positron range.

Measurements of positron range have shown that this distribution consists of a central spike (fwhm < 0.5 mm) plus tails that can extend outward for several mm [40, 67-70]. See Table 1 for values of the fwhm, the fw(0.1)m, and the effective fwhm *r* for four important positron emitters. The fwhm and fw(0.1)m describe the narrow central region of the distribution, but not the tails. The rms reflects the statistical broadening of the entire range distribution. The quantity *r* is defined as 2.35 × rms so that combining it in quadrature with other fwhm values is equivalent to combining all the rms values in quadrature and then multiplying by 2.35 to convert to an overall fwhm.

Table 1.
Positron range factors for four isotopes. From ref. [69].

Isotope	^{18}F	^{11}C	^{68}Ga	^{82}Rb
Max β^+ energy (MeV)	0.64	0.96	1.90	3.35
fwhm (mm)	0.13	0.13	0.31	0.42
fw(0.1)m (mm)	0.38	0.39	1.6	1.9
r = 2.35 × rms (mm)	0.54	0.92	2.8	6.1

Individual photodetectors vs. light sharing photodetectors.

We have analyzed [71] published resolution measurements from 7 tomographs using crystals individually coupled to photodetectors [14, 24, 28, 29, 40, 49, 58] and 10 tomographs using light-sharing block detectors [41-43, 51-53, 56, 61, 62]. For the 7 individually coupled systems, the combined effects of detector crystal width, annihilation photon non-collinearity, source size, and the reconstruction process yield predictions that are slightly less than the reported resolutions (Figure 2). The additional factors required for agreement have an average of only 0.3 mm. The 10 block detector systems require additional factors that have an average of 2.0 mm fwhm, assumed to be due to a combination of Compton scatter in the block, statistical fluctuations in the photomultiplier tube signals, and imperfections in the block decoding scheme (Figure 3). Monte Carlo simulations show that positioning errors caused by Compton scatter within the block only account for only 0.9 mm of the degradation in resolution [71] .

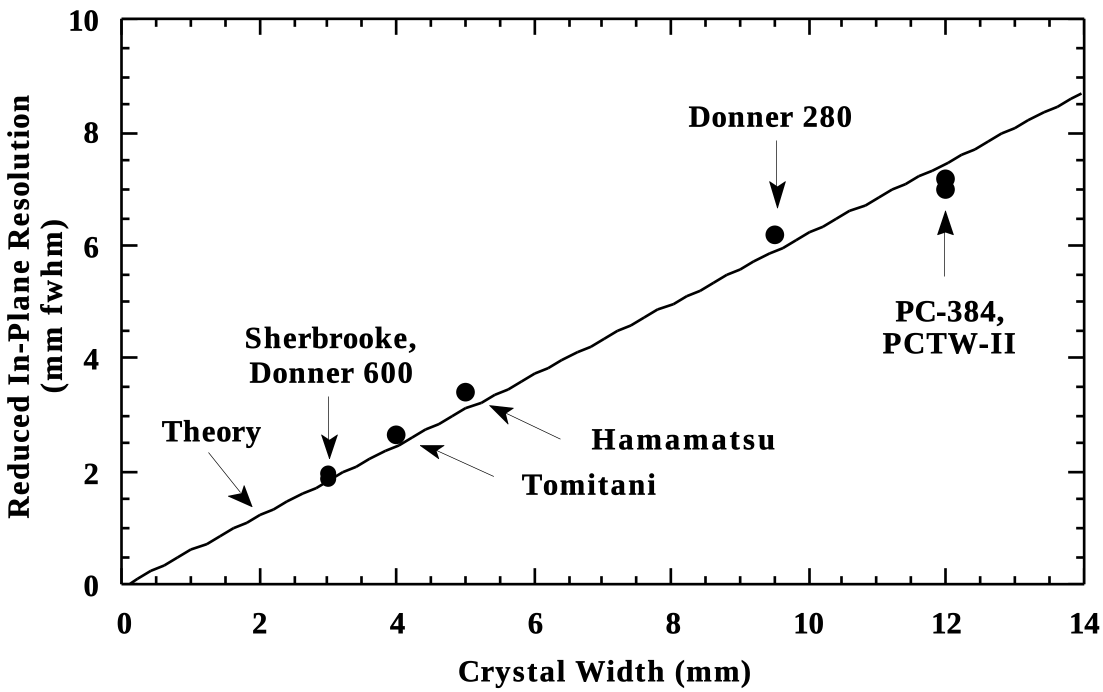

Figure 2.
In-plane resolution (fwhm mm) vs. crystal width for six positron tomographs with individual crystal- phototube coupling. Annihilation noncollinearity and source size contributions have been mathematically removed. Sherbrooke ref. [58]; Donner 600 ref. [40]; Tomitani ref. [29]; Hamamatsu ref. [49]; Donner 280 ref. [14]; PC-384 ref. [24]; PCTW-II ref. [28].

Combined formula for reconstructed image resolution.

Combining these factors, we describe the combined reconstructed image resolution Γ, as influenced by detector size d, noncollinearity (through the detector array diameter D), the effective positron range r, and an additional factor

b (such as that contributed by a block decoding scheme). Table 2 shows that it is possible to achieve <2 mm resolution for ^{18}F, assuming that b is zero.

$$\Gamma = 1.25\sqrt{(d/2)^2 + (0.0022D)^2 + r^2 + b^2}$$

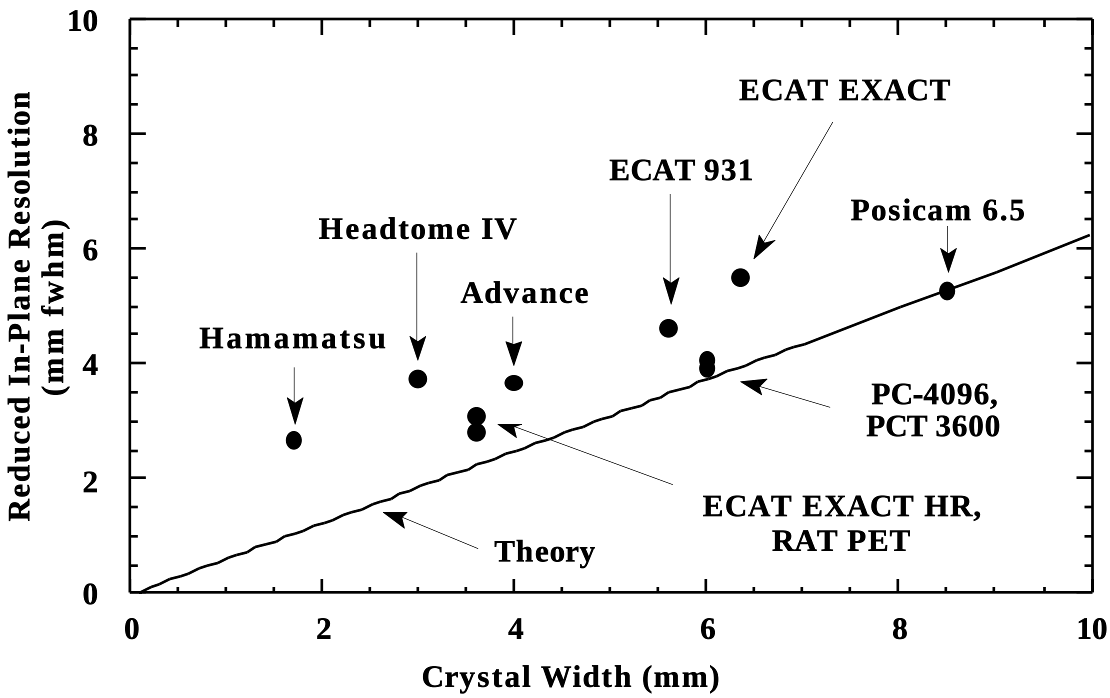

Figure 3.
In-plane resolution (fwhm mm) vs. crystal width for seven positron tomographs with block ratio crystal- phototube coupling. Annihilation noncollinearity and source size contributions have been mathematically removed. Hamamstsu ref. [52]; Headtome IV ref. [43]; ECAT EXACT HR ref. [61]; RAT PET ref. ???; Advance ref. [62]; ECAT 931 ref. [41]; PC-4096 ref. [42]; PCT 3600 ref. [53]; ECAT EXACT ref. [56]; Posicam 6.5 [51].

Table 2.

Reconstructed image resolution Γ (fwhm mm) for several values of detector ring diameter D and detector size d, assuming ^{18}F (r = 0.54 mm) and individual coupling (b = 0).

d (mm) =	6	4	3	2	1.5	1
D = 60 cm	4.15	3.07	2.59	2.18	2.01	1.89
D = 45 cm	4.01	2.87	2.35	1.88	1.69	1.54
D = 30 cm	3.90	2.72	2.16	1.64	1.42	1.24
D = 20 cm	3.85	2.65	2.07	1.52	1.28	1.07

Improved scintillators.

The availability of a scintillator with a higher light output than BGO, such as LSO ($Lu_2(SiO_4)O:Ce$) [72-75] would improve the resolution of the light sharing block detector and may reduce the value of *b* in the spatial resolution equation above.

Depth of interaction measurement.

An additional issue in high resolution PET is detector penetration, which causes radial blurring at points distant from the central axis of the tomograph. This effect is eliminated most efficiently by measuring of the depth of interaction in the detector for determination of the true line of position [76-81]. In some cases, this would allow a reduction in the detector diameter, reducing the effect of noncollinearity on spatial resolution, and reduce the number of detectors, which would reduce the cost of the tomograph.

SENSITIVITY FACTORS

Detector stopping power.

As described earlier, high detection sensitivity is enhanced by using dense detectors with high atomic number, particularly in high resolution tomographs employing small crystals.

Axial field of view and optimal inter-plane septa.

Detection sensitivity is also enhanced by using a large number of detector rings. Ideally, events should be accepted from the entire volume of interest. Removing or retracting the inter-plane septa can increase the angular acceptance, but also increases prompt scatter and random backgrounds. The tradeoffs, advantages, and disadvantages of retracting the septa have been the subject of work by a number of research groups [82-85]. While full inter-place shielding is sub-optimal due to the low solid angle acceptance, the complete removal of the shielding may be sub-optimal due to the errors and statistical fluctuations caused by the prompt scatter and random backgrounds. In that case, additional work will be required to determine the optimum shielding configuration. Use of a luminous, dense scintillator such as LSO would permit scatter rejection on an event-by-event basis, as has been demonstrated for NaI(Tl) [38].

Maximum event rate capability.

The maximum event rate is limited fundamentially by the area and dead time of the individual detector modules but also can be limited by the speed of the coincidence and address logic electronics. There is a critical need in PET for a scintillator with a decay time significantly shorter than the 300 ns of BGO, such as LSO or $PbSO_4$ [86, 87]

Increased effective sensitivity using time-of-flight information

Using time-of-flight information to localize the annihilation along the line between the two coincident detectors has several advantages [12, 15, 18, 23, 88-91]:

- The image can be reconstructed with less statistical noise
- Each annihilation can be placed near the image plane where it occurred

- Angles can be grouped, which reduces the task of data storage and tomographic reconstruction

The sensitivity advantage of time-of-flight information is described by the formula $f = L/(15\,\Delta T)$, where L is the size of the emission region and ΔT is the time-of-flight resolution fwhm [92, 93]. For a typical head image, L = 15 cm, and a timing resolution ΔT = 0.2 ns, the sensitivity advantage is 5.

NEW DEVELOPMENTS IN INSTRUMENTATION

Phototube/silicon photodiode PET detector module.
The idea of using solid state photodetectors for reading out arrays of small scintillation crystals has been under development for several years [48, 76, 94-102]. Figure 4 shows an expanded view of a proposed PET module [103]. Each optically isolated 3 × 3 × 30 mm BGO crystal is attached to a 25 mm square photomultiplier tube, which provides a timing pulse and energy discrimination, and to a photodiode, which identifies the crystal of interaction. By making the surfaces of the BGO crystals “lossy,” it is possible to use the ratio of light detected in the photodiode and photomultiplier tube to determine the depth of interaction in the crystal (Figure 5) [104]. Figure 5 shows the ratio of the photodiode pulse height to the sum of the pulse heights. The detector module was cooled to –20° to reduce electronic noise and increase the BGO signal. The phototube pulses were normalized to minimize the depth dependence of the sum. The errors in the pulse height ratio translate to an uncertainty in the depth coordinate ranging from 5 mm to 8 mm fwhm, which is sufficient to nearly eliminate the radial blurring in a head tomograph with a 60 cm diameter detector ring.

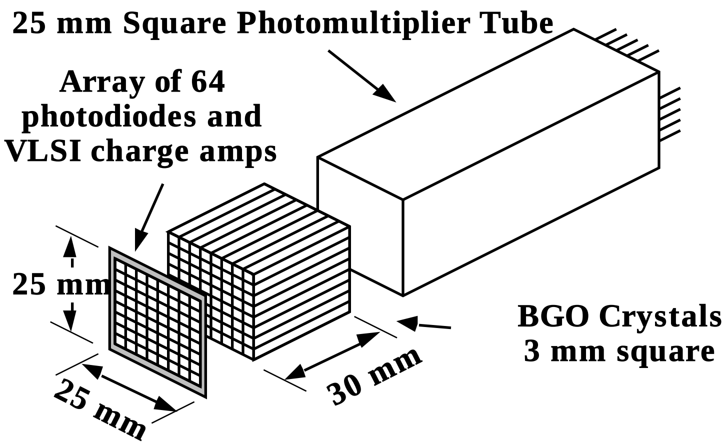

Figure 4.
A PET detector module using an array of silicon photodiodes for crystal identification and a single phototube for timing information. See text for details.

New scintillators.
We suggest that the ideal PET scintillator would have the following properties:

1 High atomic number (such as Bi or Pb) and density >6 gm/cm^3 for good photoelectric stopping power.

2 Ce activator luminescence having ≥20,000 photons per 511 keV (similar to LSO), a decay time of about 30 ns, and a wavelength between 400 and 500 nm. This luminescence is similar to that of Ce-doped LSO and would provide good pulse height resolution and low deadtime.

3 Cross luminescence having >500 photons per 511 keV, decay time <0.5 ns, and a convenient wavelength (250-500 nm) for photomultiplier tubes. This would provide good time-of-flight information. For such rapid decay times the phototube response has been be the limiting factor, but recent advances have made photomultiplier tubes available with a single photoelectron transit time jitter as low as 200 ps.

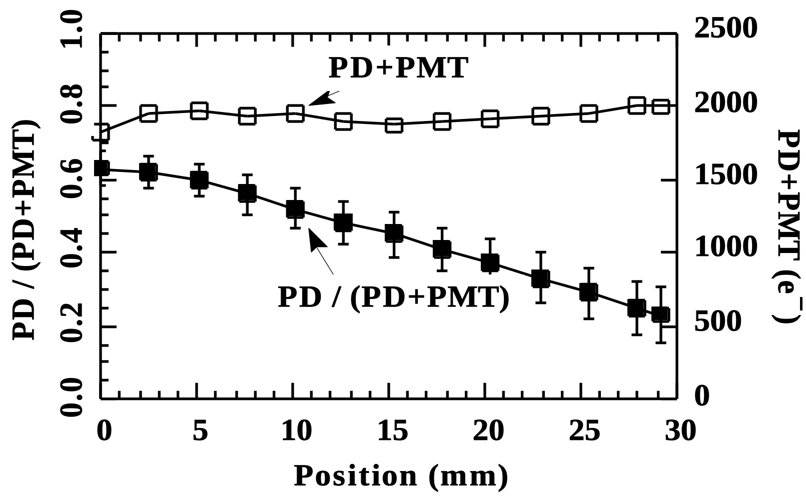

Figure 5.
Centroid of the ratio PD / (PD+PMT) as a function of excitation position. The error bars denote the width (fwhm) of this ratio. Also shown is the center of the 511 keV photopeak observed in the PD+PMT sum.

We have been searching for such scintillators for time-of-flight PET, using both synchrotron x-radiation [105-107] and a newly developed pulsed x-ray system [108, 109]. These techniques were developed for screening compounds in powdered form and measuring their fluorescent decay properties The light-sensitive x-ray tube used in the pulsed x-ray system is shown in Figure 6. Figure 7 shows an impulse response, determined by coupling a laser diode (103 ps fwhm pulse width) directly to a microchannel phototube (51 ps fwhm single photon response) [110]. We are continuing to work on our pulse discrimination to remove the satellite peak that occurs 350 ps after the main peak.

Figure 8 shows the fluorescent lifetime spectra from a powdered sample of CuI [110], which was previously reported as an ultra-fast scintillator, along with Yb_2O_3 and $BaCl_2$ [105]. The luminosity of powdered CuI is about 7% that of BGO, or about 300 photons per 511 keV. It's fitted decay time of 163 ps would yield an initial intensity of 1.8 photons/511 keV/ps. The comparable number for the fast component of BaF_2 is 1.2 photons/511 keV/ps. The fluorescence of CuI is dominated by a single ultra-fast component, the emission wavelength is convenient (430 nm), and the density is 5.62. This material may become important for the detection of high energy gamma rays, and where high counting rate and excellent timing resolution are of paramount consideration. The photoelectric stopping power is probably too low for time-of-flight PET, however. This compound is neither an alkali halide nor an alkali-earth halide, which opens the possibility that some lead or bismuth compounds might also have comparably fast fluorescent emissions.

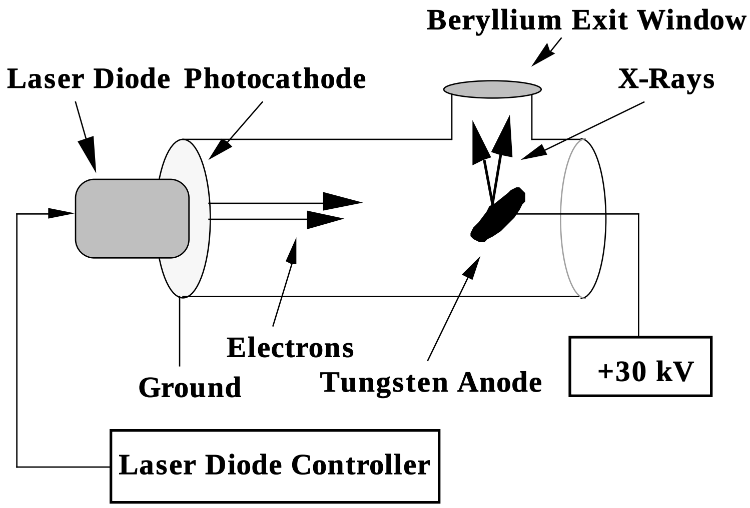

Figure 6.
Pulsed x-ray source. Brief (100 ps) bursts of light from the laser diode generate pulses of photoelectrons. These are accelerated though 30 kV to strike an anode and produce pulses of x-rays.

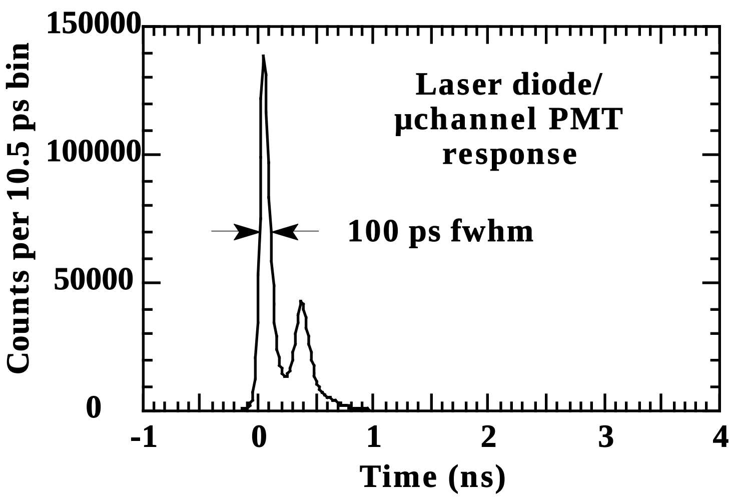

Figure 7.
Impulse response of pulsed x-ray system. Laser diode coupled directly to microchannel phototube.

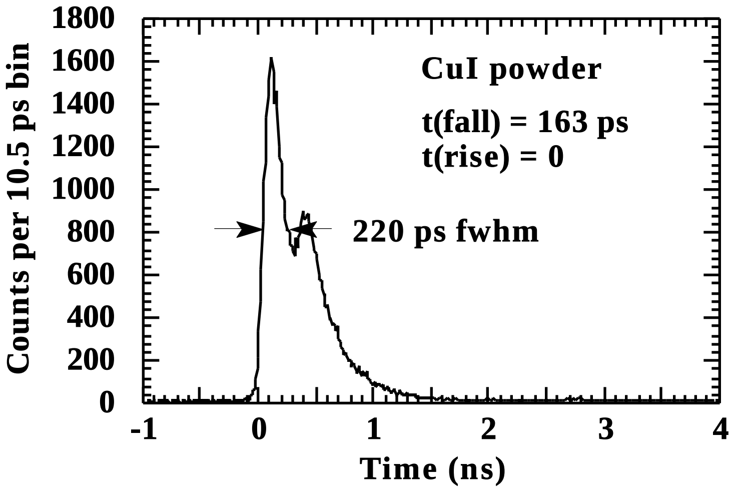

Figure 8.
Fluorescence time spectrum of CuI powder measured with pulsed x-ray system.

CONCLUSIONS

1 The ultimate spatial resolution requires small detectors with good photo-electric stopping power, either individual readout or high luminosity, and the ability to measure depth-of-interaction.

2 Maximum axial coverage requires a detector design that permits close packing and an acceptable cost per unit area.

3 Maximum quantitative accuracy requires good detection efficiency, high spatial resolution, optimum inter-plane shielding, high maximum event rates, and time-of-flight information.

4 Improved scintillators, solid-state photodetector arrays, and photomultiplier tubes will make all of the above goals possible.

ACKNOWLEDGMENTS

This work was supported in part by the Director, Office of Energy Research, Office of Health and Environmental Research, Medical Applications and Biophysical Research Division of the U.S. Department of Energy under contract No. DE-AC03-76SF00098, and in part by Public Health Service Grant Nos. P01 HL25840, and R01 CA48002, awarded by the National Heart Lung and Blood and National Cancer Institutes, Department of Health and Human Services. One of us (W.W. Moses) was supported in this research by the Whitaker Foundation.

REFERENCES

1 S. Rankowitz, J. S. Robertson, W. A. Higinbotham and e. al, “Positron scanner for locating brain tumors,” IRE Int Conv Rec 1962; 10 (Issue 9): 49-56.

2 C. A. Burnham and G. L. Brownell, “A multi-crystal positron camera,” IEEE Trans Nucl Sci 1972; NS-19(3): 201-205.

3 J. S. Robertson, R. B. Marr, B. Rosenblum and e. al, “Thirty-two crystal positron transverse section detector,” In: Tomographic Imaging in Nuclear Medicine. New York: Society of Nuclear Medicine, 1973; 142-153.

4 M. M. Ter-Pogossian, M. E. Phelps, E. J. Hoffman and e. al, “A positron-emission transaxial tomograph for nuclear imaging (PETT),” Radiology 1975; 114: 89-98.

5 S. E. Derenzo, H. Zaklad and T. F. Budinger, “Analytical study of a high-resolution positron ring detector system for transaxial reconstruction tomography,” J Nucl Med 1975; 16: 1166-1173.

6 Z. H. Cho, M. B. Cohen, M. Singh and e. al, “Performance and evaluation of the circular ring transverse axial positron camera (CRTAPC),” IEEE Trans Nucl Sci 1977; NS-24: 532-543.

7 N. Mullani, C. Higgins, J. Hood and C. Currie, “PETT IV: design analysis and performance characteristics,” IEEE Trans Nucl Sci 1978; NS-25: 180-183.

8 C. Bohm, L. Eriksson, M. Bergström and e. al, “A computer assisted ring detector positron camera system for reconstruction tomography of the brain,” IEEE Trans Nucl Sci 1978; NS-25: 624-637.

9 G. L. Brownell, J. A. Correia and R. G. Zamenhof, “Positron instrumentation,” In: Recent Advances in Nuclear Medicine, Grune and Straton, NY. 1978; 1-50.

10 N. Mullani, M. Ter-Pogossian, C. Higgins and e. al, “Engineering aspects of PETT V,” IEEE Trans Nucl Sci 1979; NS-26: 2703-2706.

11 S. E. Derenzo, T. F. Budinger, J. L. Cahoon, W. L. Greenberg, R. H. Huesman and T. Vuletich, “The Donner 280-crystal high resolution positron tomograph,” IEEE Trans Nucl Sci 1979; NS-26: 2790-2793.

12 M. M. Ter-Pogossian, N. A. Mullani, D. C. Ficke and e. al, “Photon time-of-flight-assisted positron emission tomography,” J Comput Assist Tomogr 1981; 5: 227-239.

13 I. Kanno, K. Uemura, S. Miura and e. al, “Headtome: A hybrid emission tomograph for single photon and positron emission imaging of the brain,” J Comput Assist Tomogr 1981; 5: 216-226.

14 S. E. Derenzo, T. F. Budinger, R. H. Huesman, J. L. Cahoon and T. Vuletich, “Imaging properties of a positron tomograph with 280 BGO crystals,” IEEE Trans Nucl Sci 1981; NS-28: 81-89.

15 M. M. Ter-Pogossian, D. C. Ficke, M. Yamamoto and J. T. Hood, “Design characteristics and preliminary testing of SUPER PETT I, a positron emission tomograph utilizing photon time-of-flight information (TOF PET),” Proceedings of The Workshop on Time-of-Flight Tomography, St. Louis, 1982, 37-41.

16 T. F. Budinger, S. E. Derenzo, R. H. Huesman and J. L. Cahoon, “Positron emission tomography: instrumentation perspectives,” Proceedings of The International Workshop on Physics and Engineering in Medical Imaging, Asilomar, 1982, Cat no 82CH1751-7, pp 3-13.

17 E. Tanaka, N. Nohara, T. Tomitani and M. Endo, “Analytical study of the performance of a multilayer positron computed tomography scanner,” J Comput Assist Tomogr 1982; 6: 350-364.

18 R. Gariod, R. Allemand and E. Cormoreche, "The "LETI" positron tomograph architecture and time of flight improvements," Proceedings of The International Workshop on Time-of-Flight Positron Tomography, 1982, Cat No 82CH1791-3.

19 G. Muehllehner, J. G. Colsher and R. M. Lewitt, "A hexagonal bar positron camera: problems and solutions," IEEE Trans Nucl Sci 1983; NS-30: 652-660.

20 M. Yamamoto, D. Ficke and M. Ter-Pogossian, "Performance study of PETT VI, a positron computed tomograph with 288 cesium fluoride detectors," IEEE Trans Nucl Sci 1982; NS-29: 529-533.

21 H. Murayama, N. Nohara, E. Tanaka and e. al, "A quad BGO detector and its timing and positioning discrimination for positron computed tomography," Nucl Instr Meth 1982; 192: 501-511.

22 T. F. Budinger, S. E. Derenzo and R. H. Huesman, "Instrumentation for positron emission tomography," Annals of Neurology 1984; 15: (supplement): S35-S43.

23 N. A. Mullani, J. Gaeta, K. Yerian and e. al, "Dynamic imaging with high resolution time-of-flight PET camera - TOFPET I," IEEE Trans Nucl Sci 1984; NS-31: 609-613.

24 J. Litton, M. Bergström, L. Eriksson, C. Bohm, G. Blomqvist and M. Kesselberg, "Performance study of the PC-384 positron camera system for emission tomography of the brain," Journal of Computer Assisted Tomography 1984; 8: 74-87.

25 H. Murayama, E. Tanaka, N. Nohara, T. Tomitani and M. Yamamoto, "Twin BGO detectors for high resolution positron emission tomography," Nucl Instr Meth 1984; 221: 633-640.

26 N. Nohara, E. Tanaka and T. Tomitani, "Analytical study of performance of high resolution positron emission computed tomographs for animal study," IEEE Trans Nucl Sci 1985; NS-32: 818-821.

27 L. Eriksson, C. Bohm, M. Kesselberg, J. E. Litton, M. Bergström and G. Blomquist, "A high resolution positron camera," In: The Metabolism of the Human Brain Studied with Positron Emission Tomography. New York: Raven Press, 1985; 33-46.

28 K. Okajima, K. Ueda, K. Takami and e. al, "Performance study of the whole-body, multilayer positron computed tomograph –PCTW–II–," IEEE Trans Nucl Sci 1985; NS-32: 902-906.

29 T. Tomitani, N. Nohara, H. Murayama, M. Yamamoto and E. Tanaka, "Development of a high resolution positron CT for animal studies," IEEE Trans Nucl Sci 1985; NS-32: 822-825.

30 K. Uemura, I. Kanno, S. Miura and e. al, "High resolution positron tomograph: HEADTOME III: system description and preliminary report on the performances," In: The Metabolism of the Human Brain Studied with Positron Emission Tomography. New York: Raven Press, 1985; 47-56.

31 T. F. Budinger and R. H. Huesman, "Ten precepts for quantitative data acquisition and analysis," Circulation 1985; 72 Suppl. IV: 53.

32 M. E. Casey and R. Nutt, "A multicrystal two dimensional BGO detector system for positron emission tomography," IEEE Trans Nucl Sci 1986; NS-33: 460-463.

33 S. E. Derenzo, “Recent developments in positron emission tomography (PET) instrumentation,” In: Physics and Engineering of Computerized Multidimensional Imaging and Processing. 1986; SPIE Vol. 671, pp 232-243.

34 Y. Hirose, I. Kanno, S. Yamamoto, M. Amano, S. Miura, H. Iida and K. Uemura, “A stationary high resolution positron emission tomograph HEADTOME IV: Design and preliminary data,” J Nucl Med 1987; 28: 607.

35 S. E. Derenzo, R. H. Huesman, J. L. Cahoon, A. Geyer, D. Uber, T. Vuletich and T. F. Budinger, “Initial results from the Donner 600 crystal positron tomograph,” IEEE Trans Nucl Sci 1987; NS-34: 321-325.

36 C. A. Burnham, D. E. Kaufman, D. A. Chesler, C. W. Stearns, D. R. Wolfson and G. L. Brownell, “Cylindrical PET detector design,” IEEE Trans Nucl Sci 1988; NS-35: 675-679.

37 K. Shimizu, T. Ohmura, M. Watanabe, H. Uchida and T. Yamashita, “Development of 3-D detector system for positron CT,” IEEE Trans Nucl Sci 1988; NS-35: 717-720.

38 G. Muehllehner, J. S. Karp, D. A. Mankoff, D. Beerbohm and C. E. Ordonez, “Design and performance of a new positron tomograph,” IEEE Trans Nucl Sci 1988; NS-35: 670-674.

39 T. K. Lewellen, A. N. Bice, R. L. Harrison, M. D. Pencke and J. M. Link, “Performance measurements of the SP3000/UW time-of-flight positron emission tomograph,” IEEE Trans Nucl Sci 1988; NS-35: 665-669.

40 S. E. Derenzo, R. H. Huesman, J. L. Cahoon, A. B. Geyer, W. W. Moses, D. C. Uber, T. Vuletich and T. F. Budinger, “A positron tomograph with 600 BGO crystals and 2.6 mm resolution,” IEEE Trans Nucl Sci 1988; NS-35: 659-664.

41 T. J. Spinks, T. Jones, M. C. Gilardi and J. D. Heather, “Physical performance of the latest generation of commercial positron scanner,” IEEE Trans Nucl Sci 1988; NS-35: 721-725.

42 S. Holte, L. Eriksson, J. E. Larsson, T. Ericson, H. Stjernberg, P. Hansen, C. Bohm, M. Kesselberg and e. al, “A preliminary evaluation of a positron camera system using weighted decoding of individual crystals,” IEEE Trans Nucl Sci 1988; NS-35: 730-734.

43 S. Yamamoto, H. Iida, M. Amano, S. Miura, Y. Hirose and I. Kanno, “In-plane resolution characteristics for a positron emission tomograph: Headtome IV,” IEEE Trans Nucl Sci 1989; NS-36: 1003-1005.

44 H. Iida, S. Miura, I. Kanno, M. Murakami and e. al, “Design and evaluation of Headtome-IV, a whole-body positron emission tomograph,” IEEE Trans Nucl Sci 1989; NS-36: 1006-1010.

45 J. G. Rogers, R. Harrop, G. H. Coombes and e. al, “Design of a volume-imaging positron emission tomograph,” IEEE Trans Nucl Sci 1989; NS-36: 993-997.

46 P. Schotanus, C. W. E. v. Eijk and R. W. Hollander, “A new gamma camera for positron emission tomography,” IEEE Trans Nucl Sci 1989; NS-36: 1090-1094.

47 P. E. Valk, W. J. Jagust, S. E. Derenzo, R. H. Huesman, A. B. Geyer and T. F. Budinger, “Clinical evaluation of a high-resolution (2.6-mm) positron emission tomograph,” Radiology 1990; 176: 783-790.

48 R. Lecomte, J. Cadorette, A. Jouan and e. al, “High resolution positron emission tomography with a prototype camera based on solid state scintillation detectors,” IEEE Trans Nucl Sci 1990; NS-37: 805- 811.

49 T. Yamashita, H. Uchida, H. Okada, T. Kurono, T. Takemori, M. Watanabe and e. al, “Development of a high resolution PET,” IEEE Trans Nucl Sci 1990; NS-37: 594-599.

50 T. Yamashita, M. Watanabe, K. Shimizu and H. Uchida, “High resolution block detectors for PET,” IEEE Trans Nucl Sci 1990; NS-37: 589-593.

51 N. A. Mullani, K. L. Gould, R. K. Hartz, R. E. Hitchens, W. H. Wong, D. Bristow, S. Adler, E. A. Philippe and e. al, “Design and performance of Posicam 6.5 BGO positron camera,” J Nucl Med 1990; 31: 610-616.

52 H. Saji, Y. Magáta, Y. Yonekura, N. Tamaki, T. Sasayama, J. Konishi, A. Yokoyama and e. al, “Performance characteristics of newly developed positron emission tomography system for animal studies,” J Nucl Med (abstract) 1991; 32: 1064-1065.

53 M. Endo, H. Fukuda, T. Suhara, T. Matsumoto, T. Iinuma, T. Yamasaki and e. al, “Design and performance of PCT-3600W (15-slice type): a whole-body positron emission tomograph,” J Nucl Med (abstract) 1991; 32: 1061.

54 T. F. Budinger, S. E. Derenzo, R. H. Huesman, W. J. Jagust and P. E. Valk, “High resolution positron emission tomography for medical science studies,” Acta Radiologica Supplementum 1991; 376: 15-23.

55 S. Rajeswaran, W. F. Jones, L. G. Byars, J. Young, C. W. Williams, M. Andreaco, S. P. Hume, A. A. Lammertsma and T. Jones, “Physical characteristics of a small diameter positron emission tomograph,” IEEE Nuclear Science Symposium Conference Record 92CH3232-6 1992; 2: 985-987.

56 K. Wienhard, L. Eriksson, S. Grootoonk, M. Casey, U. Pietrzyk and W.-D. Heiss, “Performance evaluation of a new generation PET,” J Nucl Med (abstract) 1992; 33: 861.

57 K. Wienhard, M. Dahlbom, L. Eriksson, C. Michel, U. Pietrzyk and W.-D. Heiss, “Comparitive performance evaluation of the ECAT EXACT and ECAT EXACT HR positron cameras,” Annals Nucl Med 1993; 7 (supplement): 68- 69.

58 C. Marriott, J. Cadorette, R. Lecomte, V. Scasnar, J. Rousseau and J. E. v. Lier, “High resolution positron emission tomograph with solid state detectors: an *in vivo* demonstration,” J Nucl Med (abstract) 1993; 34: 101P.

59 W. Robeson, V. Dhawan, S. Takikawa, B. Babchyck, I. Zanzi and e. al, “Superpett 3000 time-of-flight PET tomograph: optimization of factors affecting quantitation,” IEEE Trans Nucl Sci 1993; 40: 135- 142.

60 R. Freifelder, A. T. Haigh and J. S. Karp, “Reducing edge effects and improving position resolution in position sensitive NaI(Tl) detectors,” IEEE Trans Nucl Sci 1993; NS-40: 208- 213.

61 K. Wienhard, M. Dahlbom, L. Eriksson, C. Michel, U. Pietrzyk and W.-D. Heiss, “Performance evaluation of the high resolution PET scanner ECAT EXACT HR,” J Nucl Med (abstract) 1993; 34: 101P.

62 T. R. DeGrado, T. G. Turkington, J. J. Williams, C. W. Stearns, J. M. Hoffman and R. E. Coleman, “Performance characteristics of a new generation PET scanner,” J Nucl Med (abstract) 1993; 34: 101P.
63 M. J. Weber and R. R. Monchamp, “Luminescence of $Bi_4Ge_3O_{12}$: spectral and decay properties,” J Appl Phys 1973; 44: 5495-5499.
64 Z. H. Cho and M. R. Farukhi, “Bismuth germanate as a potential scintillation detector in positron cameras,” J Nucl Med 1977; 18: 840-844.
65 M. J. Weber, “Discovery of the scintillation properties of BGO: underlying principles,” Proceedings of The International Workshop on Bismuth Germanate, Princeton University, 1982, 3-20.
66 P. Colombino, B. Fiscella and L. Trossi, “Study of positronium in water and ice from 22 to –144°C by annihilation quantum measurements,” Nuovo Cimento 1965; 38: 707-723.
67 Z. H. Cho, J. Chan, L. Eriksson and e. al, “Positron ranges obtained from biomedically important positron-emitting radionuclides,” J Nucl Med 1975; 16: 1174-1176.
68 S. E. Derenzo, “Precision measurement of annihilation point spread distributions for medically important positron emitters,” In: Positron Annihilation. Sendai, Japan: The Japan Institute of Metals, 1979; 819-823.
69 S. E. Derenzo, “Mathematical removal of positron range blurring in high resolution tomography,” IEEE Trans Nucl Sci 1986; NS-33: 565-569.
70 S. F. Haber, S. E. Derenzo and D. Uber, “Application of mathematical removal of positron range blurring in positron emission tomography,” IEEE Trans Nucl Sci 1990; NS-37: 1293-1299.
71 W. W. Moses and S. E. Derenzo, “Empirical observation of resolution degradation in positron emission tomographs utilizing block detectors,” J Nucl Med (abstract) 1993; 34: 101P.
72 C. L. Melcher and J. S. Schweitzer, “Cerium-doped lutetium orthosilicate: a fast, efficient new scintillator,” IEEE Trans Nucl Sci 1992; NS-39: 502- 505.
73 H. Suzuki, T. A. Tombrelloo, C. L. Melcher and J. S. Schweitzer, “Light emission mechanism of $Lu_2(SiO_4)O$:Ce,” IEEE Nuclear Science Symposium Conference Record 92CH3232-6 1992; 1: 120- 122.
74 C. L. Melcher, “LSO/photodiode and LSO/avalanche photodiode detectors,” IEEE Nuclear Science Symposium Conference Record 92CH3232-6 1992; 1: 123- 125.
75 F. Daghighian, P. Shenderov, K. S. Pentlow, M. C. Graham, C. L. Melcher and J. S. Schweitzer, “Evaluation of cerium doped lutetium oxyorthosilicate (LSO) scintillation crystal for PET,” IEEE Nuclear Science Symposium Conference Record 92CH3232-6 1992; 2: 876- 878.
76 S. E. Derenzo, T. F. Budinger and T. Vuletich, “High resolution positron emission tomography using narrow bismuth germanate crystals and individual photosensors,” IEEE Trans Nucl Sci 1983; NS-30: 665-670.
77 J. S. Karp and M. E. Daube-Witherspoon, “Determination of depth-of-interaction in scintillation crystals using a temperature gradient,” Nucl Instr Meth 1987; A260: 509-517.

78 W. W. Moses and S. E. Derenzo, “Effect of depth-of-interaction measurement resolution on radial elongation in PET (reviewed abstract),” J Nucl Med 1990; 31: 749.

79 W. W. Moses, R. H. Huesman and S. E. Derenzo, “A new algorithm for using depth-of-interaction measurement information in PET data acquisition (reviewed abstract),” J Nucl Med 1991; 32: 995.

80 R. S. Miyaoka, T. K. Lewellen and A. N. Bice, “Development of a high resolution PET detector module with depth of interaction information,” IEEE Nuclear Science Symposium Conference Record 92CH3232-6 1992; 2: 933- 935.

81 T. A. DeVol, W. W. Moses and S. E. Derenzo, “Monte Carlo optimization of depth-of-interaction resolution in PET crystals,” IEEE Trans Nucl Sci 1993; NS-40: 170- 174.

82 C. J. Thompson, “The effect of collimation on scatter fraction in multi-slice PET,” IEEE Trans Nucl Sci 1988; NS-35: 598-602.

83 C. J. Thompson, “The effect of collimation on singles rates in multi-slice PET,” IEEE Trans Nucl Sci 1989; NS-36: 1072-1077.

84 M. Dahlbom, S. R. Cherry, L. Eriksson, E. J. Hoffman and K. Wienhard, “Optimization of PET instrumentation for brain activation studies,” IEEE Nuclear Science Symposium Conference Record 92CH3232-6 1992; 2: 853-858.

85 D. W. Townsend, “Three dimensional PET: The current status and future prospects,” Annals Nucl Med 1993; 7 (supplement): 1- 2.

86 F. W. K. Firk, “A comparative study of the scintillation response of natural crystals of anglesite ($PbSO_4$) and cerussite ($PbCO_3$),” Nucl Instr Meth 1990; A297: 532-533.

87 W. W. Moses, S. E. Derenzo and P. Schlichta, “Scintillation properties of lead sulfate,” Trans Nucl Sci 1992; NS-39: 1190-1194.

88 N. Mullani, J. Markham and M. Ter-Pogossian, “Feasibility of time-of-flight reconstruction in positron emission tomography,” J Nucl Med 1980; 21: 1095-1097.

89 N. Mullani, W. Wong, R. Hartz and e. al, “Sensitivity improvement of TOFPET by the utilization of the inter-slice coincidences,” IEEE Trans Nucl Sci 1982; NS-29: 479-483.

90 T. K. Lewellen, R. L. Harrison and A. N. Bice, “An experimental evaluation of the effect of time-of-flight information in image reconstruction for the Scanditronix/PETT Electronics SP-3000 positron emission tomograph — preliminary results.,” IEEE Trans Nucl Sci 1989; NS-36: 1095-1099.

91 M. Yamamoto, N. Nohara, E. Tanaka, T. Tomitani and e. al, “Time-of-flight positron imaging and the resolution improvement by an iterative method,” IEEE Trans Nucl Sci 1989; NS-36: 998-1002.

92 S. E. Derenzo, “Comparison of detector materials for time-of-flight positron tomography,” Proceedings of The International Workshop on Time-of-Flight Positron Tomography, St. Louis, MO, 1982, Cat No 82CH1791-3, pp 63-68.

93 A. Mallon, P. Grangeat and P. X. Thomas, “Comparison between three-dimensional positron emission tomography with and without time-of-flight

measurement," IEEE Nuclear Science Symposium Conference Record 92CH3232-6 1992; 2: 988- 990.

94 J. S. Iwanczyk, J. B. Barton, A. J. Dabrowski and e. al, "A novel radiation detector consisting of an HgI_2 photodetector coupled to a scintillator," IEEE Trans Nucl Sci 1983; NS-30: 363-367.

95 J. B. Barton, E. J. Hoffman, J. S. Iwanczyk and e. al, "A high-resolution detection system for positron tomography," IEEE Trans Nucl Sci 1983; NS-30: 671-675.

96 D. E. Groom, "Silicon photodiode detection of bismuth germanate scintillation light," Nucl Instr Meth 1984; 219: 141-148.

97 S. E. Derenzo, "Initial characterization of a BGO-silicon photodiode detector for high resolution PET," IEEE Trans Nucl Sci 1984; NS-31: 620-626.

98 S. E. Derenzo, "Gamma-ray spectroscopy using small, cooled bismuth germanate scintillators and silicon photodiodes," Nucl Instr Meth 1984; 219: 117-122.

99 G. A. Petrillo, R. J. McIntyre, R. Lecomte and e. al, "Scintillation detector with large-area reach-through avalanche photodiodes," IEEE Trans Nucl Sci 1984; NS-31: 417-423.

100 M. Dahlbom, M. A. Mandelkern, E. J. Hoffman and e. al, "Hybrid mercuric iodide (HgI_2) – gadolinium orthosilicate (GSO) detector for PET," IEEE Trans Nucl Sci 1985; NS-32: 533-537.

101 R. Lecomte, D. Schmitt, A. W. Lightstone and e. al, "Performance characteristics of BGO-silicon avalanche photodetectors for PET," IEEE Trans Nucl Sci 1985; NS-32: 482-486.

102 C. Carrier, C. Martel, D. Schmitt and R. Lecomte, "Design of a high resolution positron emission tomograph using solid state scintillation detectors," IEEE Trans Nucl Sci 1988; NS-35: 685-690.

103 W. W. Moses, S. E. Derenzo, R. Nutt, W. M. Digby, C. W. Williams and M. Andreaco, "Performance of a PET detector module utilizing an array of silicon photodiodes to identify the crystal of interaction," IEEE Trans Nucl Sci (in press) 1993; NS-40:

104 W. W. Moses and S. E. Derenzo, "Design studies for a PET detector module using a PIN photodiode to measure depth of interaction," IEEE Trans Nucl Sci (in preparation) 1994; NS-41:

105 S. E. Derenzo, W. W. Moses, J. L. Cahoon, T. A. DeVol and L. A. Boatner, "X-ray fluorescence measurements of 412 inorganic compounds," IEEE Nuclear Science Symposium Conference Record 91CH3100-5 1991; 1: 143- 147.

106 S. E. Derenzo, W. W. Moses, R. Perera, J. Litton and J. Cahoon, "Prospects for new inorganic scintillators," IEEE Trans Nucl Sci 1990; NS-37: 203-208.

107 S. E. Derenzo and W. W. Moses, "Experimental efforts and results in finding new heavy scintillators," Proceedings of The CRYSTAL 2000: International workshop on heavy scintillators for scientific and industrial applications, Chamonix, France, 1992, pp 11.

108 S. E. Derenzo, W. W. Moses, S. C. Blankespoor, M. Ito and K. Oba, "Design of a pulsed x-ray system for fluorescent lifetime measurements with a timing resolution of 109 ps," IEEE Nuclear Science Symposium Conference Record 92CH3232-6 1992; 1: 117- 119.

109 S. C. Blankespoor, S. E. Derenzo, W. W. Moses, M. Ito and K. Oba, “Characterization of a pulsed X-ray source for fluorescent lifetime measurements,” IEEE Trans Nucl Sci (in preparation) 1994; NS-41:

110 S. E. Derenzo, W. W. Moses and S. C. Blankespoor, “High resolution fluorescent time spectra of six ultra-fast powdered inorganic scintillators,” IEEE Trans Nucl Sci (in preparation) 1994; NS-41: